Global sensitivity analysis and calibration of parameters for a physically-based agro-hydrological model

Xu Xu [a, b, *], Chen Sun [c], Guanhua Huang [a, b, **], Binayak P. Mohanty [d]

[a] Chinese-Israeli International Center for Research and Training in Agriculture, China Agricultural University, Beijing, 100083, PR China
[b] Center for Agricultural Water Research, China Agricultural University, Beijing, 100083, PR China
[c] Institute of Environment and Sustainable Development in Agriculture, Chinese Academy of Agricultural Sciences, Beijing, 100081, PR China
[d] Biological and Agricultural Engineering, Texas A&M University, College Station, TX, 77843, USA

ARTICLE INFO

ABSTRACT

Efficient parameter identification is an important issue for mechanistic agro-hydrological models with a complex and nonlinear property. In this study, we presented an efficient global methodology of sensitivity analysis and parameter estimation for a physically-based agro-hydrological model (SWAP-EPIC). The LH-OAT based module and the modified-MGA based module were developed for parameter sensitivity analysis and inverse estimation, respectively. In addition, a new solute transport module with numerically stable schemes was developed for ensuring stability of SWAP-EPIC. This global method was tested and validated with a two-year dataset in a wheat growing field. Fourteen parameters out of the forty-nine total input parameters were identified as the sensitive parameters. These parameters were first inversely calibrated by using a numerical case, and then the inverse calibration was performed for the real field experimental case. Our research indicates that the proposed global method performs successfully to find and constrain the highly sensitive parameters efficiently that can facilitate application of the SWAP-EPIC model.

© 2016 Elsevier Ltd. All rights reserved.

1. Introduction

Agro-hydrological models have been an important tool for supporting decision making in the development of agricultural water management strategies. Since the physical description and prediction of hydrological, chemical and biological processes at field by some physically-based or mechanistic models are highly valuable, these models, such as SWAP (van Dam et al., 1997) and HYDRUS (Šimůnek et al., 1997), are frequently used. Most of them are based on the numerical solution of Richards equation for variably saturated water flow and on analytical or numerical solution of advection-dispersion equation. Compared with the simple models (i.e. using lumped or tipping-bucket approach, e.g. SIM-dualKc, AquaCrop, CERES and EPIC), these mechanistic models can simulate multi-processes of soil water flow, solute and heat transport, and crop growth in great detail, and be suitable for some more complicated conditions (Ranatunga et al., 2008; van Dam et al., 2008; Xu et al., 2013). However, these models often contain more number of parameters, and have complex, dynamic, and nonlinear properties. Moreover, more functions have been added involving hysteresis, mobile-immobile flow, macropore flow, multi-species transport and reaction, and so on. These may result in a more severe problem of over-parameterization. Hence, the parameter identification becomes a major and urgent problem for agro-environmental prediction and future model use (Ines and Mohanty, 2008; Wöhling et al., 2008; Della Peruta et al., 2014). An efficient identification of the sensitive and important parameters and the subsequent parameter estimation would be very helpful for the future use of physically-based agro-hydrological models.

Parameter sensitivity analysis (SA) is a prerequisite step in the model-building process (Campolongo et al., 2007). The SA method identifies parameters that do or not have a significant impact on model simulation of real world observations for specific farmlands (van Griensven et al., 2006) and is critical for reducing the number of parameters required in model validation (Hamby, 1994).

Generally, SA can be divided into two different schools: the local SA school and the global one (Saltelli et al., 1999). In the first approach, the local response of model output is obtained by varying the parameters one at a time while holding the others fixed to certain nominal values. This approach has been adopted by some studies because of its easy application. Yet, local SA methods have the known limitations of linearity and normality assumptions and local variations. For complex non-linear models, only global sensitivity analysis (GSA) methods are able to provide relevant information on the sensitivity of model outputs to the whole range of model parameters (Varella et al., 2010). In recent years, many studies have focused on the GSA methods for identifying the important parameters as well as distinguishing the effects of different input conditions (Wesseling et al., 1998; Cariboni et al., 2007; Saltelli and Annoni, 2010; DeJonge et al., 2012; Zhao et al., 2014; Neelam and Mohanty, 2015; Hu et al., 2015; Pianosi et al., 2015). Typical successful applications include the methods of RSA (Yang, 2011), extended FAST (Varella et al., 2010), Sobol' (Nossent et al., 2011) and LH-OAT (van Griensven et al., 2006) in the related hydrological and crop models. The choice of the sample size and of the threshold for the identification of insensitive input factors was also preliminarily investigated for GSA methods (Yang, 2011; Sarrazin et al., 2016). Although different sensitivity techniques exist, each of them would result in a slightly different sensitivity ranking for the important parameters near the top of the ranking list. In general, the practicality of the method depends on the calculation ease and the desired usefulness of results (Hamby, 1994).

Parameter estimation is an essential way of calibrating a model, which is also important to the accurate prediction of agro-hydrological processes. Different approaches have been applied and may be classified as two main types, i.e., trial-and-error method (manual) and inverse optimization method (automatic). The former has been widely applied because of its simple concept and easy application (Xu et al., 2013). It is very suitable to the simple models with less parameters and complexity, such as when applying to the SimDualKc and AquaCrop models (Paredes et al., 2014). However, the trial-and-error method is often cumbersome and time-consuming when applying to the physically mechanistic models, especially for layered soil-profile and complicated field conditions (Jacques et al., 2002). Hence, in addition to the subjectivity of the trial-and-error method, there have also been a large number of research studies on its alternative: automatic inverse optimization approaches for model calibration. These algorithms may be classified as local and global search methods. The local method, using an iterative search starting from a single arbitrary initial point, may often prematurely terminate the search and therefore present a lower chance to find a single unique solution, such as the well-known Gauss-Marquardt-Levenberg algorithm used by PEST (Wöhling et al., 2008; Malone et al., 2010). This inspires the application of global parameter estimation (GPE) methods in the field of vadose zone hydrology, e.g., genetic algorithms (Ines and Droogers, 2002; Ines and Mohanty, 2008; Shin et al., 2012), ant-colony optimization (Abbaspour et al., 2001), Ensemble Kalman Filter (Evensen, 2003) and shuffled complex methods (Duan et al., 1994). In the past, the inverse optimization of parameters of soil hydraulic properties as well as the related well-posedness, uniqueness and the stability are extensively studied related to the physically-based models (Kool et al., 1987; Šimůnek and van Genuchten, 1996; Ines and Droogers, 2002; Shin et al., 2012). The inverse estimation of root water uptake parameters is also carried out (Hupet et al., 2003). In contrast, very few research studies extend to simultaneously consider the solute fate simulation and its parameter estimation (Jacques et al., 2002; Xu et al., 2012). Note that they are of importance for the accurate agro-hydrological modeling in salt-affected irrigated areas, where the ignorance of solute transport would lead to errors in the inverse parameter estimation. Uncertainty analysis is also applied in watershed hydrological modeling (Yang et al., 2008), but only a few cases are related to the detailed and complicated field scale studies (Shin et al., 2012; Shafiei et al., 2014).

To our knowledge, few studies have reported the development of both parameter sensitivity analysis and inverse estimation for the complicated physically-based agro-hydrological models. The general purpose of this study was to investigate the global method of sensitivity analysis in conjunction with inverse parameter estimation for effectively identifying parameters of a mechanistic agro-hydrological model (SWAP-EPIC). SWAP-EPIC is modified version of the well-known SWAP model, proposed by Xu et al. (2013). A GSA module and a GPE module were respectively developed for SWAP-EPIC model to perform sensitivity analysis and estimation of model parameters. An efficient Latin Hypercube One-factor-At-a-Time (LH-OAT) method was adopted to construct the GSA module. The GPE module was then developed based on the genetic algorithm (GA). Meanwhile, to avoid the problem of numerical instability, a new solute transport module was developed with the fully implicit and Crank-Nicholson difference schemes. Finally, the proposed global method for sensitivity analysis and parameter estimation was tested and verified using the field experiment datasets in Huinong experimental site, Qingtongxia Irrigation District of the upper Yellow River basin, Northwest China. The methodology described in this study would help increase the efficiency of parameter identification for the complicated agro-hydrological model and would also help understand the relationship between different processes.

2. Materials and methods

2.1. Model description

2.1.1. Agro-hydrological simulation model: updated SWAP-EPIC

By coupling the SWAP (Soil-Water-Atmosphere-Plant) model (Kroes and van Dam, 2003) and the EPIC crop growth module (Williams et al., 1989), Xu et al. (2013) proposed an agro-hydrological simulation model SWAP-EPIC. This model had been used to evaluate soil water flow, solute transport, crop growth, and water productivity in Heihe River basin (Jiang et al., 2015) and Yellow River basin (Xu et al., 2013, 2015). However, based on our experience, the numerical solution of solute transport is not stable enough in original SWAP-EPIC with the explicit finite-difference scheme, because the time step should meet the stability criterion for ensuring stability (van Genuchten and Wierenga, 1974). When the size of time step exceeds a limit and stability criterion is not satisfied, the numerical errors in the solution are amplified as the time marches forward, leading to an invalid or unstable solution (Zheng and Bennett, 2002). According to our experience, this caused very large numerical errors and mass imbalance for salinity problems in SWAP-EPIC, which was prone to happen in GSA and GPE modeling with a large range of parameter changes (Xu et al., 2012, 2013). Subsequently, it would lead to the crash of GSA simulation and efficiency reduction for GPE simulation. Therefore, in this study, we developed a new solute transport module optionally using the fully implicit or Crank-Nicholson finite-difference scheme to replace the original one in the updated version of SWAP-EPIC. It could indeed improve the model stability and make the calculation much faster. Main processes of the modified SWAP-EPIC model are described below.

Soil water flow

Soil water flow is based on the one-dimensional (1-D) Richards equation for vertical flow:

$$C(h)\frac{\partial h}{\partial t} = \frac{\partial}{\partial z}\left[K(h)\left(\frac{\partial h}{\partial z} + 1\right)\right] - S(h), \tag{1}$$

where C is the differential soil water capacity (cm^{-1}), h is the soil water pressure head (cm), t is time (d), z is the vertical coordinate (cm, positive upward), K is the hydraulic conductivity $(cm\ d^{-1})$ and S is the soil water extraction rate by plant roots $(cm^3\ cm^{-3}\ d^{-1})$. This equation is solved using an implicit finite-difference scheme in water flow module, which is from the original SWAP model. Eq. (1) requires knowledge of the soil hydraulic properties, which are described by the van Genuchten (1980) and Mualem (1976) functions, respectively:

$$S_e(h) = \frac{\theta(h) - \theta}{\theta_s - \theta_r} = \frac{1}{(1 + |\alpha h|^n)^{1-1/n}}, \tag{2}$$

$$K(h) = K_s S_e^\lambda \left[1 - \left(1 - S_e^{n/(n-1)}\right)^{1-1/n}\right]^2, \tag{3}$$

in which S_e is the effective saturation, θ_r and θ_s denote the residual and saturated water contents $(cm^3\ cm^{-3})$, respectively, K_s is the saturated hydraulic conductivity $(cm\ d^{-1})$, $\alpha\ (cm^{-1})$ and $n\ (-)$ are empirical shape parameters, and λ is a pore connectivity/tortuosity parameter $(-)$. A variable active-node method is added for simulating the soil water flow during melting period (Xu et al., 2013).

Solute transport

For solute transport, the advection−dispersion equation (ADE) (Boesten and van der Linden, 1991) is applied as follows:

$$\frac{\partial(\theta c + \rho_b Q)}{\partial t} = -\frac{\partial qc}{\partial z} + \frac{\partial}{\partial z}\left[\theta\left(D_{dif} + D_{dts}\right)\frac{\partial c}{\partial z}\right] - \mu(\theta c + \rho_b Q) - K_r S c, \tag{4}$$

where c is the solute concentration in the soil liquid phase $(g\ cm^{-3})$, ρ_b is the dry soil bulk density $(g\ cm^{-3})$, Q is the adsorbed concentration $(g\ g^{-1})$, q is the Darcian velocity $(cm\ d^{-1})$, D_{dif} is the diffusion coefficient $(cm^2\ d^{-1})$, D_{dis} is the dispersion coefficient $(cm^2\ d^{-1})$, μ is the first-order rate coefficient of transformation (d^{-1}), and K_r is the root uptake preference factor $(-)$. An explicit, central finite difference scheme is used to solve Eq. (4) in the original SWAP-EPIC model. It has the advantage that incorporation of the nonlinear adsorption, mobile/immobile concepts, and other non-linear processes is relatively easy (Kroes and van Dam, 2003). However, as mentioned before, the explicit scheme may have some stability problems for the GSA and GPE modeling due to the time step required to satisfy the stability criterion, which also sacrifices computation time. Thus, in this study, the Eq. (4) was numerically solved by developing the fully implicit and the Crank-Nicholson finite-difference schemes in time discretization within a new solute transport module. Grid Peclet number and Courant number were used together to ensure the numerical stability.

Evaporation and transpiration

The upper boundary conditions are defined by the actual evaporation and transpiration rates, and the irrigation and precipitation fluxes. The potential evapotranspiration $(ET_p, cm\ d^{-1})$ is estimated by the Penman-Monteith equation (Monteith, 1965) using daily meteorological data of solar radiation as computed from sunshine duration, air temperature, relative humidity and wind speed as well as crop parameters. The ET_p is then partitioned into potential soil evaporation $(E_p, cm\ d^1)$ and potential crop transpiration $(T_p, cm\ d^1)$ using the leaf area index (LAI). In dry soil conditions, the maximum evaporation rate, $E_{max}\ (cm\ d^1)$, is calculated according to Darcy's law (van Dam et al., 1997). As the actual soil evaporation $(E_a, cm\ d^1)$ may be overestimated using Darcy's law, a two-stage evaporation model, recommended by FAO (Allen et al., 1998), is introduced to correct E_p to $E_{ats}\ (cm\ d^1)$ in the updated SWAP-EPIC model. This new evaporation model is added because the two empirical power functions of Black et al. (1969) and Boesten and Stroosnijder (1986) in original SWAP have also led to an incorrect estimation of E_a under shallow water table conditions. Finally, the actual evaporation $(E_a, cm\ d^1)$ rate is determined by taking the minimum value of E_{max} and E_{ats}.

The actual transpiration $(T_a, cm\ d^1)$ is governed by the root water uptake (S) which is calculated from the potential transpiration, rooting depth and distribution, and a possible reduction due to water and salt stress. In SWAP-EPIC, the S-shaped function incorporating a salinity threshold value, proposed by Dirksen and Augustijn (1988) is used for describing the water or salinity stress, which is based on the soil solution osmotic head instead of EC_e. The minimal crop resistance $(r_c, s\ m^{-1})$ is assumed a constant value in the original SWAP; however, it is known that r_c is affected by vapor pressure deficit (VPD, kPa) and atmospheric CO_2 level. Therefore, the methods proposed by Easterling et al. (1992) and Stockle et al. (1992) were incorporated to make a correction of r_c related to VPD and CO_2 concentration in this study.

Crop growth

SWAP-EPIC includes the conceptual module of the EPIC crop growth model (Williams et al., 1989). This module considers leaf area development, light interception, and the conversion of intercepted light into biomass and yield together with effects of temperature, water and salt stress. Biomass is computed from the solar radiation intercepted by the crop leaf area, which is estimated with Beer's law (Monsi and Saeki, 1953). The potential increase in biomass on a given day is estimated as a function of the plant radiation-use efficiency with consideration of stress factors such as water, salinity, and temperature (Monteith and Moss, 1977). Radiation-use efficiency is estimated using the approach proposed by Stockle et al. (1992).

Leaf area index (LAI) is computed for the various phenological development stages considering heat units accumulation (Williams et al., 1989). LAI represents the level of canopy cover, and is estimated as a function of heat units, crop stress, and development stages. Crop height is estimated as such in the EPIC model (Williams et al., 1989). The fraction of total biomass partitioned to the root system is 30−50% in seedlings and reduces to 5−20% in mature plants (Jones, 1985). This model decreases the fraction of total biomass in roots linearly from 0.4 at emergence to 0.2 at maturity, which is similar to the EPIC model (Williams et al., 1989). The root depth generally increases rapidly from planting to a specific maximum depth by early mid-season (Borg and Grimes, 1986). The vertical root distribution in the soil profile is assumed as a piecewise-linear function of the root depth. The actual crop yield is calculated using the harvest index concept following the EPIC model procedures (Williams et al., 1989), i.e., as a function of the above ground biomass $(kg\ ha^{-1})$ and environmental stresses (soil temperature, soil salinity, fertilizers, etc.).

2.1.2. Sensitivity analysis and parameter estimation

Two new modules (GSA and GPE) were developed and embedded into SWAP-EPIC for effective identification of model parameters. The GSA module for sensitivity analysis was based on the LH-OAT method which had a sampling strategy that was a combination of Latin Hypercube (LH) and One-factor-At-a-Time (OAT) sampling. The genetic algorithm based method was adopted here to construct the GPE module for inverse parameter estimation. The calculation procedure for model calibration with GSA and GPE modules is explained in Fig. 1.

Sensitivity analysis: LH-OAT method

The LH-OAT method has a sampling strategy that is a combination of Latin Hypercube and One-factor-At-a-Time sampling. It allows performing GSA for a long list of parameters with less computational cost (van Griensven et al., 2006). It starts with dividing the parameter range into N equal intervals, and taking N LH sampling points for each parameter. Random values of the parameters are generated, with each interval to be sampled only once. Then each of the N LH sampling is varied for P times by changing each of the P parameters one at a time, using the OAT design. Thus it only requires a total of $N \times (P+1)$ model runs. A final sensitivity index S_i for the ith parameter is calculated by averaging the partial effects for all Latin Hypercube points, as follows:

$$S_i = \frac{1}{N} \sum_{j=1}^{N} \left| \frac{\frac{M(e_{1,j},...,e_{i,j}(1+f_i),...,e_{p,j}) - M(e_{1,j},...,e_{i,j},...,e_{p,j})}{[M](e_{1,j},...,e_{i,j}(1+f_i),...,e_{p,j}) + M(e_{1,j},...,e_{i,j},...,e_{p,j})/2}}{f_i} \right|, \quad (5)$$

where $M(\cdot)$ refers to the model functions, f_i is the fraction by which the parameter e_i is changed (a predefined constant), and j refers to a LH point. GSA result is obtained according to S_i value, with largest value being given rank 1 and the smallest value being given a rank equal to the total number of parameters analyzed. The default value of f_i is set to 5%.

In this paper, the above LH-OAT sampling method was applied and embedded into SWAP-EPIC as a new module for GSA. A restricted set of parameters was applied in sensitivity analysis for capturing the major processes described in agro-hydrological simulation. These parameters can be selected for GSA as required, and their ranges were needed and often determined based on the existing literature. For example, Table 1 presents the selected parameters and their ranges for the case studies in this paper. In the GSA module, parameters were classified into five categories related to different processes (soil water flow, solute transport, crop growth, and water or salt stress of root water uptake). The model outputs could be optionally selected as objective variables as necessary, including actual evapotranspiration (ET_a), LAI, bottom flux (Q_{bot}), dry above ground biomass (D-AGB), and layer-specific soil moisture and salinity concentration.

Parameter calibration: genetic algorithm based method

The genetic algorithms (GAs) are global and robust methods for searching the optimum solution to the complex problems, using the precept of natural selection (Holland, 1975; Goldberg, 1989). GA consists of three basic operators of selection, crossover and mutation. It represents a solution using strings (referred as chromosomes) of variables (represented as genes) in a search problem. The search will start by initializing a population of chromosomes. Each chromosome is evaluated on its performance
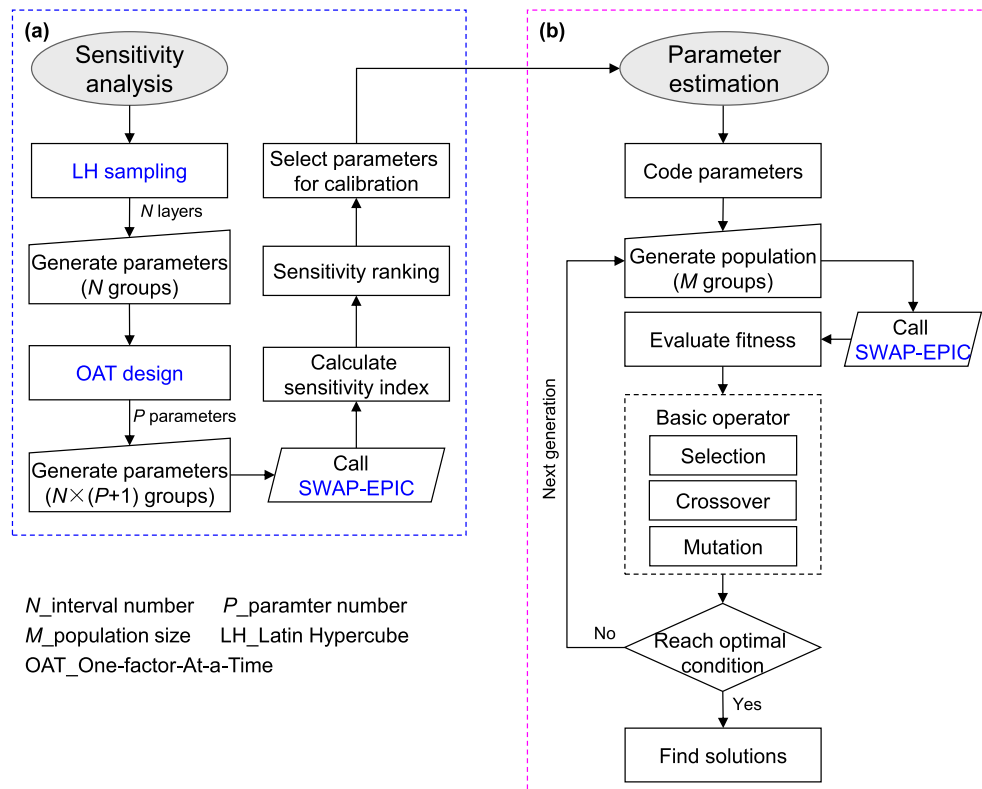

Fig. 1. Schematic diagram of global sensitivity analysis (a) and inverse estimation (b) of parameters for agro-hydrological model (SWAP-EPIC) using LH-OAT and modified-MGA methods, respectively.

Table 1
Parameters and their ranges used in sensitivity analysis in the case study.

Parameter	Definition[a]	Min	Max	Process
θ_{ri}	Saturated water content for material i (cm³ cm⁻³)	0	0.05	Soil water flow
θ_{si}	Residual water contents for material i (cm³ cm⁻³)	0.36	0.52	Soil water flow
K_{si}	Saturated hydraulic conductivity for material i (cm d¹)	5	50	Soil water flow
α_i	Empirical shape parameter in Eq. (2) for material i (−)	0.005	0.03	Soil water flow
λ_i	Pore connectivity/tortuosity parameter in Eq. (3) for material i (−)	−6	0	Soil water flow
n_i	Empirical shape parameter in Eq. (2) for material i (−)	1.15	1.8	Soil water flow
L_{dis}	Dispersion length (cm)	5	22	Solute transport
D_w	Solute diffusion coefficient in free water (cm² d⁻¹)	0	10	Solute transport
h_1	No water extraction at higher pressure heads (cm)	−10	0	Water stress of root uptake
h_{2u}	h below which optimum water uptake starts for top layer (cm)	−50	−11	Water stress of root uptake
h_{2l}	h below which optimum water uptake starts for sub layer (cm)	−50	−11	Water stress of root uptake
h_3	h below which water uptake reduction starts at high atmospheric demand (cm)	−400	−700	Water stress of root uptake
h_4	h below which water uptake is zero (cm)	−18,000	−7000	Water stress of root uptake
r_s	Minimum crop resistance (s m⁻¹)	50	80	Crop growth
a_{ic}	Empirical coefficient of rainfall interception (cm d¹)	0.1	0.5	Crop growth
P_2	Exponential coefficient of S-Shape salt stress function (−)	1	2.5	Salt stress of root uptake
h_{50c}	Osmotic head at which water uptake is reduced by 50% (cm)	−9500	−6000	Salt stress of root uptake
h_{cr}	Threshold value of Osmotic head (cm)	−5000	−3000	Salt stress of root uptake
T_b	Minimum temperature for plant growth (ºC)	0	4	Crop growth
T_{opt}	Optimal temperature for plant growth (ºC)	18	24	Crop growth
DLAI	Fraction of growing season controlled by cumulative temperature when leaf area index starts declining (−)	0.48	0.7	Crop growth
RLAD	Leaf area index decline rate (−)	0.4	2	Crop growth
L_{max}	Maximum leaf area index (−)	5	7	Crop growth
PHU	Total potential heat units required for crop maturation (ºC)	1800	2200	Crop growth
c_{drain}	solute concentration in groundwater (g L⁻¹)	0	6	Solute transport

[a] Note: subscript i is the number of soil material for parameters in the top six rows, and equal to 1–5 in the case.

using a fitness function. On the basis of the performance, the chromosomes are selected into the mating pool to form the offspring through the crossover and mutation of genes. Selection, crossover, and mutation are repeated for many generations for reproducing the chromosome that fit the environment best. The best chromosome would represent the optimal or near optimal solution to the search problem (Carroll, 1998; Goldberg, 2002). In this study, the modified-MGA has been adopted to calibrate the model parameters by minimizing the error between simulated and observed data. The uniqueness of modified-MGA is the ability to restart when the chromosomes of the micropopulation are nearly 90% similar in structure (Ines and Droogers, 2002; Shin et al., 2012).

The modified-MGA code (Carroll, 1998; Ines and Droogers, 2002) was integrated as a GPE module for parameter estimation into SWAP-EPIC by embedded coupling. The highly sensitive parameters selected by LH-OAT method were adopted to be calibrated here. Their range and classification were set as same in SA (Table 1). Similar to the sensitivity analysis, the model outputs could be optionally selected as objective variables according to the observation data collected. On the basis of these objective variables, the fitness function was constructed using the weighted average method, as follows:

$$fitness(j) = \sum_{k=1}^{m} \omega_k \left(\frac{1}{\frac{1}{n_k} \sum_{i=1}^{n_k} |x_{sim} - x_{obs}|_i} \right), \qquad (6)$$

where $fitness(j)$ is the fitness value of the jth chromosome, x_{sim} and x_{obs} are the normalized values of simulated and observed objective variables, respectively (−), the subscript i donates the ith observation, the n_k is the number of observations for the kth objective variable, m is the number of total selected objective variables, and ω_k is the weighting factor for the kth objective variable (−) with $\sum_{k=1}^{m} \omega_k$ equals to one.

When GA approaches to the solution, the fitness values of most chromosomes in a population may be close. To avoid the non-uniqueness and instability in the inverse solution, a kind of uncertainty bounds to solution was created analogous to that used by Abbaspour et al. (2004) or Shin et al. (2012). The inverse modeling was conducted with a multi-population generated by various random generator seeds. The average fitness of all chromosomes was calculated and classified as above or below average at the end of searching. The above average solutions were

Table 2
Soil physical properties of experimental area.

Soil depths (cm)	Soil particle size distribution (%)			Soil texture	Bulk density (g cm⁻³)	Field capacity (−11 kPa)	Wilting point (−1500 kPa)
	Sand (2.0–0.05 mm)	Silt (0.05–0.002 mm)	Clay (<0.002 mm)				
0–30	55.9	39.3	4.8	Sandy loam	1.41	0.28	0.059
30–81	54.0	41.0	5.0	Loam	1.60	0.31	0.068
81–103	55.0	41.3	3.7	Loam	1.52	0.28	0.072
103–140	21.5	74.7	3.8	Silty loam	1.55	0.36	0.120
140–150	71.0	27.0	2.0	Sandy loam	1.58	0.32	0.106

Table 3
Values of the van Genuchten-Mualem model parameters and dispersion length for different soil layers, calibrated by Xu et al. (2013).

Depths (cm)	Layer and soil type	θ_s (cm³ cm⁻³)	θ_r (cm³ cm⁻³)	α (cm⁻¹)	n (−)	λ (−)	K_s (cm d¹)	L_{dis} (cm)
0−30	1 Sandy loam	0.40	0.02	0.020	1.40	0.5	6.0	19
30−81	2 Loam	0.42	0.02	0.015	1.39	0.5	13.0	
81−103	3 Loam	0.38	0.01	0.018	1.32	0.5	10.0	
103−140	4 Silty loam	0.45	0.01	0.013	1.26	0.5	7.0	
>140	5 Sandy loam	0.41	0.01	0.020	1.25	0.5	10.0	

considered as the most probable solutions, which were used respectively to run the model. Then, the 95 percent confidence interval (95PCI) of outputs with the probable solutions was calculated for each observation time. The upper and lower 95PCI was the range of output, which may represent some modeling uncertainties.

2.2. Model test: new solute transport module

The developed new solute transport module was tested by using an analytical solution with steady-state water flow condition. Only the result of fully implicit scheme was selected and exemplified in this study. The solution of 1-D analytical solute transport models for the third-type (i.e. flux-type) sources, first
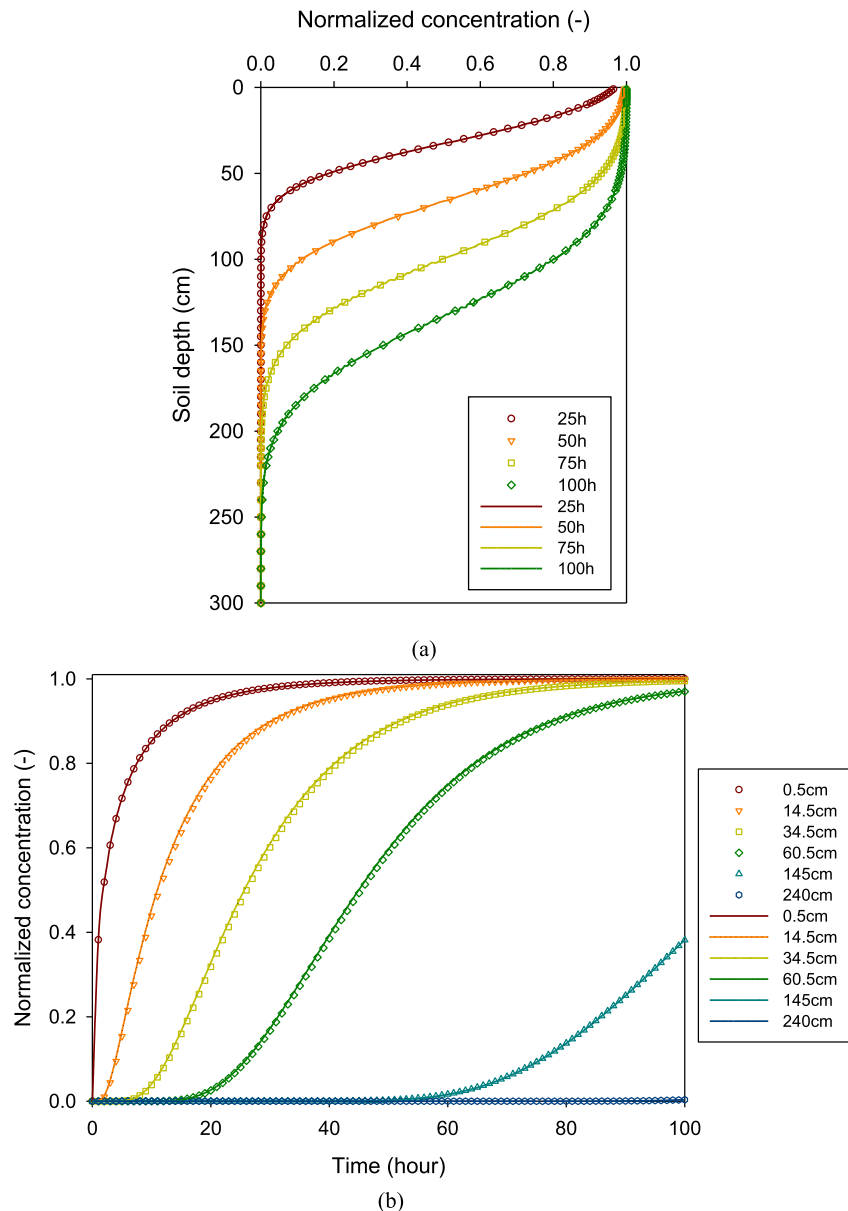

(a)

(b)

Fig. 2. Comparison of solute concentration profiles (a) at different hours and breakthrough curves (b) at different depths between the analytical solution given in Eq. (7) and the numerical solutions given SWAP-EPIC module.

obtained by Lindstrom et al. (1967), is used and presented as follows (Batu, 2005):

$$C_n(z, t) = \frac{C - C_i}{C_0 - C_i}$$
$$= \frac{1}{2}\text{erfc}\left[\frac{R_d z - Ut}{2(DR_d t)^{1/2}}\right] + \left(\frac{U^2 t}{\pi DR_d}\right)^{1/2} \exp\left[-\frac{(R_d z - Ut)^2}{4DR_d t}\right]$$
$$- \frac{1}{2}\left(1 + \frac{Uz}{D} + \frac{U^2 t}{DR_d}\right)\exp\left(\frac{Uz}{D}\right)\text{erfc}\left(\frac{R_d z + Ut}{2(DR_d t)^{1/2}}\right),$$

(7)

where $C_n(z, t)$ is the normalized concentration, C_i and C_0 are respectively the initial and boundary flux concentration (g L^{-1}), R_d is the solute retardation factor (−), D is the effective dispersion coefficient (cm^2 d^{-1}), U is the average pore-water velocity (cm d^1). The governing differential equation and related initial and boundary conditions are given in detail by Batu (2005). This third type solution includes finite length flow domains and ensures mass continuity, which is consistent with the practical conditions as well. A 300 cm long (loam) soil column was considered and simulation period was set 100 h for numerical solution. The column was discretized into 250 nodes with 1 cm thickness for the top 100 cm and 1 or 2 cm for the bottom 200 cm. The parameters related to solute transport were taken as follows: R_d = 1.25, U = 40 cm d^1, D = 10 cm^2 d^{-1}.

2.3. Global sensitivity analysis and calibration of parameters: field case study

The field experiment of spring wheat in 2007 and 2008 was selected as a case study for model testing. It was conducted at the Huinong experimental site, Qingtongxia Irrigation District, Ningxia Hui Autonomous Region, Northern China (39° 04′ N, 116° 39′ E, 1092 m altitude) during 2007 and 2008. The climate in the region is

Table 4
Sensitivity analysis ranking for 49 parameters of SWAP-EPIC model corresponding to different criteria.

Name	Global	ET_a	Q_{bot}	LAI	D-AGB	θ_1 (10–30 cm)	θ_2 (30–50 cm)	θ_3 (50–70 cm)	θ_4 (70–90 cm)	c_1 (10–30 cm)	c_2 (30–50 cm)	c_3 (50–70 cm)	c_4 (70–90 cm)
θ_{s1}	1	13	5	18	16	1	7	10	13	7	15	16	7
θ_{s2}	1	1	1	6	1	10	1	1	1	1	1	2	1
L_{dis}	1	8	13	16	13	22	23	21	24	2	2	1	2
T_b	1	10	14	1	2	20	19	24	25	14	10	5	14
θ_{s3}	2	36	32	34	41	36	39	27	2	25	31	30	16
α_1	2	4	2	9	8	2	6	4	8	10	6	7	5
α_2	2	15	6	11	7	6	2	2	3	5	3	3	6
h_{50c}	2	2	3	7	3	13	12	9	23	6	4	6	13
PHU	2	17	19	2	5	26	29	31	31	23	21	14	25
n_1	3	3	4	8	4	3	4	5	9	3	5	9	4
n_2	3	6	7	10	10	4	3	3	5	4	7	8	3
DLAI	3	24	26	3	22	30	30	35	35	29	34	33	34
K_{s2}	4	14	10	14	17	5	5	13	14	11	9	4	10
α_3	4	26	22	29	30	16	20	14	4	26	30	29	17
L_{max}	4	21	28	4	6	28	25	37	36	17	20	24	29
r_s	5	5	8	21	11	18	15	18	20	9	8	11	21
RLAD	5	18	31	5	18	27	35	39	38	31	35	36	33
K_{s3}	6	25	21	25	24	14	16	8	6	22	19	12	12
n_3	6	22	17	32	25	12	13	6	7	19	16	13	9
θ_{r2}	7	33	35	22	28	21	11	7	10	21	22	27	35
λ_2	7	16	18	23	19	7	8	17	11	16	14	18	15
h_{cr}	7	7	11	13	9	23	27	23	27	13	12	20	24
K_{s1}	8	12	12	15	14	8	9	11	21	8	13	15	11
λ_1	8	11	9	17	15	9	10	12	22	12	17	17	8
P_2	9	9	15	12	12	24	17	26	28	15	11	10	22
θ_{r1}	11	23	16	20	20	11	18	20	26	18	27	31	23
K_{s4}	12	32	23	36	34	19	22	25	12	30	26	32	27
K_{s5}	14	35	30	31	35	15	14	16	15	37	29	25	28
λ_3	15	29	34	41	29	25	21	15	18	32	28	22	26
θ_{r3}	16	39	40	42	44	50	50	36	16	50	50	40	40
n_4	17	31	29	43	36	17	24	19	17	36	24	19	20
θ_{s4}	18	37	38	30	37	34	32	34	50	39	37	34	18
D_w	18	28	37	28	31	32	34	33	37	27	18	23	19
α_4	19	34	36	39	32	29	26	22	19	35	38	28	30
h_{2u}	19	27	25	19	21	38	28	29	29	20	33	35	38
h_{2l}	19	19	20	26	23	33	31	50	39	33	25	21	36
a_{ic}	20	20	24	37	33	37	38	50	33	24	23	26	31
T_{opt}	24	41	44	24	26	39	50	50	50	38	50	50	43
θ_{r4}	27	40	27	50	39	50	50	50	50	50	40	42	39
h_1	27	30	33	27	27	50	50	28	32	34	32	43	41
θ_{s5}	28	42	41	38	43	35	37	38	34	28	50	39	32
λ_4	30	38	39	40	38	31	33	30	30	41	36	41	37
h_3	32	44	43	35	42	50	36	32	50	40	50	38	42
h_4	33	43	42	43	40	50	50	50	50	42	39	37	44
α_5	45	50	45	50	50	50	50	50	50	50	50	50	50
c_{drain}	45	50	46	50	50	50	50	50	50	50	50	50	45
θ_{r5}	50	50	50	50	50	50	50	50	50	50	50	50	50
λ_5	50	50	50	50	50	50	50	50	50	50	50	50	50
n_5	50	50	50	50	50	50	50	50	50	50	50	50	50

Note: The global rank 1 and 2–6 were categorized as the 'very important' and 'important' parameters, respectively.

arid continental and during the experimental period the average annual rainfall is 194 mm, with more than 70% of precipitation occurring between June and September. The experiment data had been used to calibrate the previous version of SWAP-EPIC by Xu et al. (2013) that presented a detail description of experiment conditions. The information related to weather, soil properties, groundwater, irrigation, cultivation practices, and observations were provided in Xu et al. (2013). Table 2 provides the main soil physical properties of the studied soil with five layers.

A soil profile with 300 cm depth was specified during simulations. It was divided into five horizon layers up to 150 cm, according

to observations (Table 2). The soil domain was further discretized into 200 compartments with 1 cm thickness for the first 100 cm and 2 cm thickness for 100−300 cm. The fully implicit difference scheme was selected. The corresponding soil hydraulic and solute transport parameters calibrated by Xu et al. (2013) are provided in Table 3. The simulation period was from mid-March to mid-July, covering the growth period of spring wheat both in 2007 and 2008. The model setup of initial and boundary conditions were kept same as in Xu et al. (2013).

In this case study, 49 parameters were initially selected for sensitivity analysis, with their ranges presented in Table 1. The
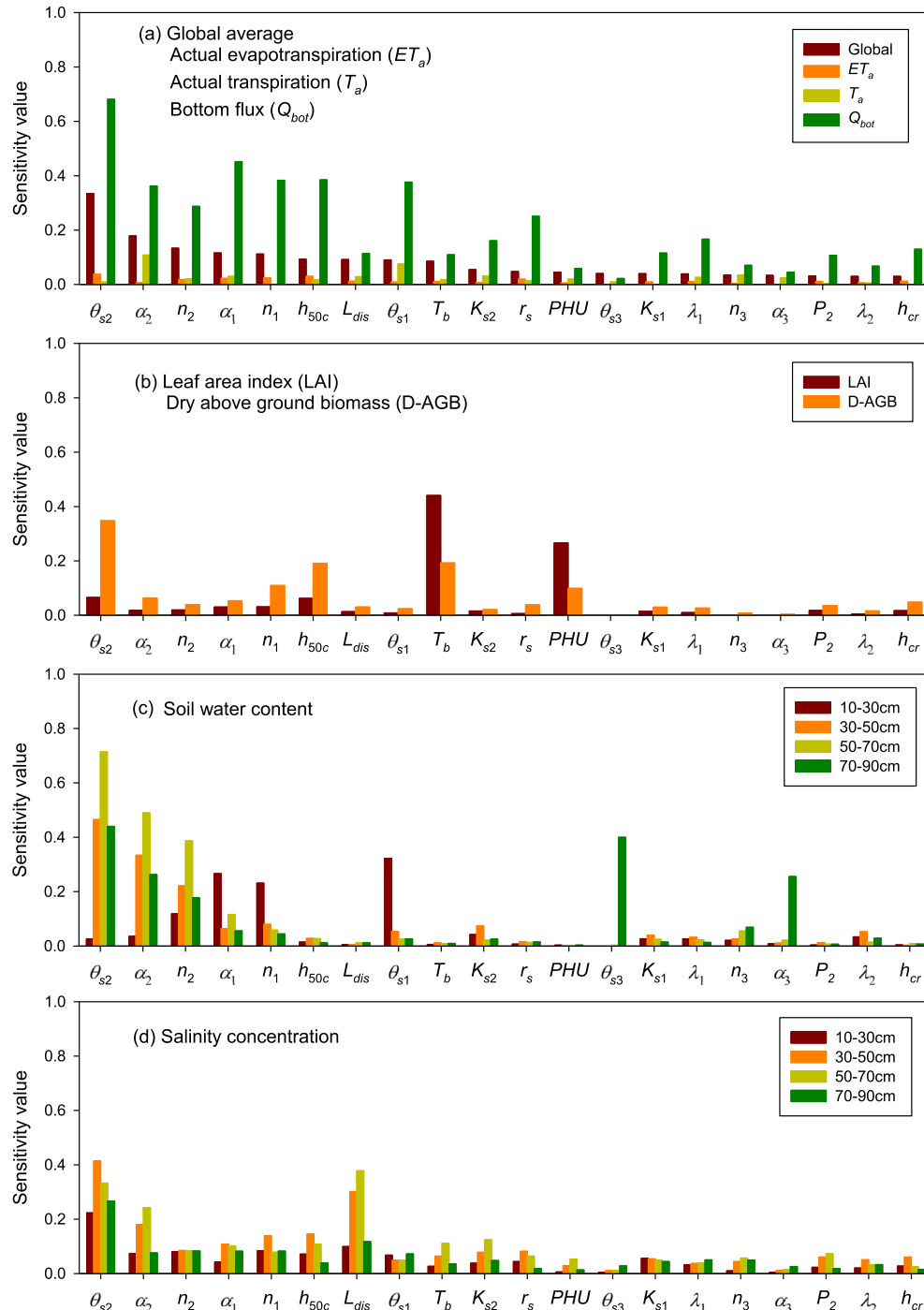

Fig. 3. Sensitivity values of the important parameters for different criteria.

Table 5
Solutions of inverse modeling for the numerical and real experimental cases using the global parameter estimation (GPE) module.

Parameter	Numerical case			Experimental case		
	Target value[a]	Average	Range	Target value	Average	Range
θ_{s1}	0.400	0.451	0.405−0.467	−	0.455	0.379−0.499
θ_{s2}	0.420	0.435	0.400−0.460	−	0.388	0.361−0.404
θ_{s3}	0.380	0.395	0.385−0.416	−	0.389	0.361−0.431
K_{s2}	13.0	23.7	5.2−43.0	−	24.9	7.1−38.5
K_{s3}	10.0	10.2	6.4−21.3	−	11.6	7.9−17.0
α_1	0.020	0.020	0.019−0.020	−	0.025	0.021−0.028
α_2	0.015	0.016	0.011−0.020	−	0.013	0.006−0.023
α_3	0.018	0.020	0.018−0.028	−	0.021	0.018−0.028
n_1	1.400	1.602	1.433−1.659	−	1.486	1.243−1.623
n_2	1.390	1.516	1.488−1.592	−	1.381	1.242−1.726
n_3	1.320	1.480	1.360−1.528	−	1.266	1.153−1.464
L_{dis}	19.0	18.2	15.8−19.2	−	19.2	10.9−21.8
r_s	70.0	70.3	63.6−74.1	−	75.2	64.6−79.8
h_{50c}	−9300	−9119	−9369~−8515	−	−9103	−9430~−8251

[a] Note: the parameter values calibrated by Xu et al. (2013) were assumed to be the real target values for the numerical case.

model outputs, including ET_a, LAI, Q_{bot}, and layer-specific soil moisture (θ_1, θ_2, θ_3 and θ_4) and salinity concentration (c_1, c_2, c_3 and c_4) for 10−30, 30−50, 50−70 and 70−90 cm layers, were selected as sensitivity criteria. The parameter sensitivity to LAI, soil moisture and salinity concentration were analyzed based on the simulated and observed data. The functions $M(\cdot)$ in Eq. (5) were constructed with the deviation between simulated and observed data. The f_i value in Eq. (5) was set equal to the default value of 5% in this study. Due to no observations of ET_a and Q_{bot}, their functions $M(\cdot)$ only

consisted of the simulated data. The sensitivity index values for each parameter were then calculated using the GSA module, and a ranking list of sensitivity was obtained. Finally, the parameter sensitivity was determined, and only highly sensitive parameters were considered for inverse calibration with the GPE module.

For evaluating the performance of the GPE module, a numerical case was adopted at first during the crop season of 2007. The model-generated output was used instead of actual field observations. The parameters calibrated by Xu et al. (2013) were considered
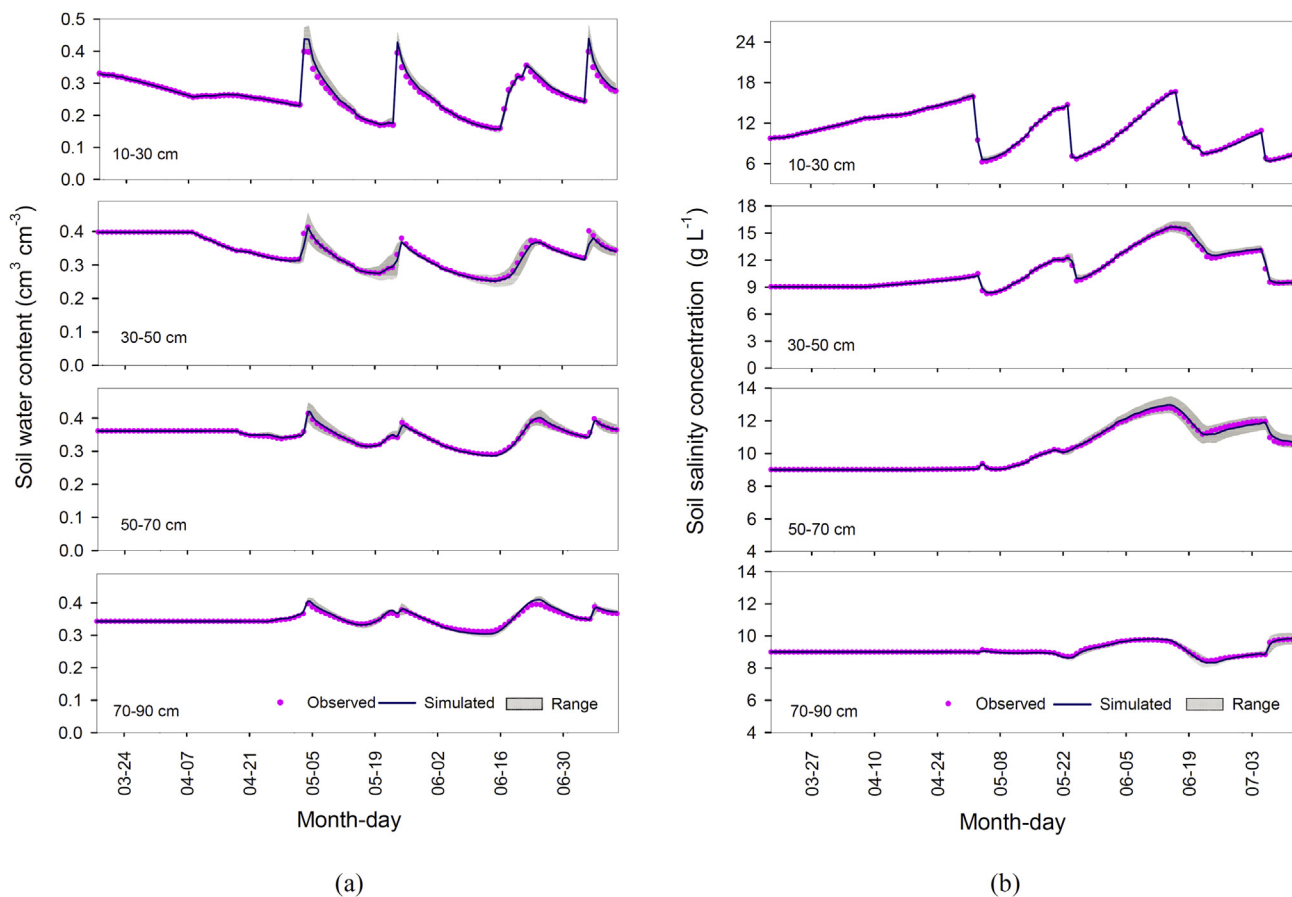

Fig. 4. Simulated versus measured soil water contents (a, at left) and salt content of the soil solution (b, at right) in different soil layers in numerical case. The solid line corresponds to the average simulation of solutions by GPE, while the gray band represents the simulation uncertainty.

for this numerical case as the real parameter values (Table 3). Running the SWAP-EPIC model with the above parameters, and the generated output was assumed as the "measured" values in the inverse modeling. The daily measured (hypothetical) ET_a, layer-specific soil moisture (θ_1, θ_2, θ_3 and θ_4) and salinity concentration (c_1, c_2, c_3 and c_4) were used to construct the fitness function (Eq. (6)). The weighting factor was respectively set to 0.20, 0.50 and 0.30. ET_a was selected as an objective because it has become a routine observation by various methods (e.g. lysimeter, eddy covariance and remote sensing).

Next, the real field measurements were used to test the applicability of GPE module (i.e. the experimental case). The fitness function for the experimental case was composed by the observed LAI, layer-specific soil moisture, and salinity concentration. The weighted factor was the same as in the numerical case with LAI instead of ET_a. The parameters were firstly calibrated though inverse modeling using the experimental data in 2007 season. Then the inverse parameters were also validated by using the observed data in 2008 season.

The mean relative error (MRE), the root mean square error (RMSE), the Nash and Sutcliffe model efficiency (NSE), the coefficient of determination (R^2) were used to quantify the model fitting performance. These indicators were defined as follows:

$$MRE = \frac{1}{N} \sum_{i=1}^{N} \frac{(P_i - O_i)}{O_i} \times 100\%, \tag{8}$$

$$RMSE = \sqrt{\frac{1}{N} \sum_{i=1}^{N} (P_i - O_i)^2}, \tag{9}$$

$$NSE = 1 - \frac{\sum_{i=1}^{N}(P_i - O_i)^2}{\sum_{i=1}^{N}\left(O_i - \overline{O}\right)^2}, \tag{10}$$

$$R^2 = \left[\frac{\sum_{i=1}^{N}\left(O_i - \overline{O}\right)\ \left(P_i - \overline{P}\right)}{\sqrt{\sum_{i=1}^{N}\left(O_i - \overline{O}\right)^2 \sum_{i=1}^{N}\left(P_i - \overline{P}\right)^2}}\right]^2, \tag{11}$$

where N is the total number of observations, P_i and O_i are respectively the ith model simulated and observed values ($i = 1, 2, …, N$), and $\overline{P}$ and $\overline{O}$ are the simulated and observed mean values, respectively. NSE = 1.0 represents a perfect fit, and negative NSE values indicate that the mean observed value is a better predictor than the simulated value (Moriasi et al., 2007). Note that when calculating the above indicators, the simulated value (P_i) corresponded to the average of simulation results obtained by all probable solutions, both for the numerical and experimental cases.

3. Results and discussion

3.1. Test of the new solute transport module

Results showed that the numerical solution with new scheme for solute transport matched very well with the analytical solution under steady-state water flow condition (Fig. 2). Fig. 2a shows a comparison between soil salinity concentration profiles calculated with analytical solution and with our numerical method at selected four times (25, 50, 75 and 100 h). Breakthrough curves at different depths (including 0.5, 14.5, 34.5, 60.5, 145 and 240 cm) are presented in Fig. 2b. The agreement was excellent. The above

comparison indicated that the numerical scheme of ADE (Eq. (4)) was correct. Thus, the new solute transport module was reasonable and accurate for solute transport modeling.

3.2. Parameter sensitivity analysis in field case study

Table 4 gives the sensitivity rank of all the parameters for different criteria (i.e. model outputs of ET_a, LAI, Q_{bot}, θ_1-θ_4 and c_1-c_4). The lowest rank from all the outputs was used to assess global parameter sensitivity as shown in the second column. Global ranks 1 were categorized as 'very important', rank 2–6 as 'important', rank 7–49 as 'slightly important' and rank 50 as 'not important'. Thus, results identified 4 very important, 15 important, 27 slightly important, and 3 not important parameters. In addition, the sensitivity values of parameters corresponding to different criteria are presented in Fig. 3.

The 4 very important parameters included θ_{s1}, θ_{s2}, L_{dis} and T_b, which covered soil water flow, solute transport and crop growth processes. The 15 important parameters mainly consisted of soil hydraulic parameters of upper two soil layers and also salt stress parameter (h_{50c}) and crop growth parameters (PHU, $DLAI$, L_{max} and $RLAD$). Some soil hydraulic parameters of upper two soil layers (including θ_{s2}, α_2, n_2, α_1, n_1 and θ_{s1}) showed important influences on all criteria (Fig. 3). It was also found that the crop growth parameters (e.g. T_b and PHU) had marked influence on LAI and biomass (Fig. 3b), but the influence was less on ET_a, soil moisture and salinity concentration (Fig. 3a,c,d). L_{dis} primarily affected the solute transports with slight sensitivity to other criteria. Results also indicated that the ET_a was not so sensitive to parameters while T_a was slightly more sensitive (Fig. 3a), under conditions of shallow water tables.

There were some soil hydraulic parameters which belonged to the 27 slightly important parameters, most of which were related to the lower two soil layers. These layers were close to groundwater table and sometimes in saturated conditions. Meanwhile, the water stress parameters were all slightly influential on all criteria, located in the lower part of ranking list (Table 4). It implied that the water supply is not insufficient under shallow water table conditions, and the root water uptake and crop growth were primarily stressed by salinity levels. This was consistent with the analysis of Xu et al. (2013). In addition, the two soil hydraulic parameters of the 5th soil layer (θ_{r5} and λ_5) caused no changes on model outputs due to the fact that this layer was saturated all the time. Overall, the GSA efficiently identified the importance of parameters and provided their sensitivity values for the SWAP-EPIC model. Besides some soil hydraulic parameters, salt stress and crop growth parameters were also significant to model output. Many of soil hydraulic parameters
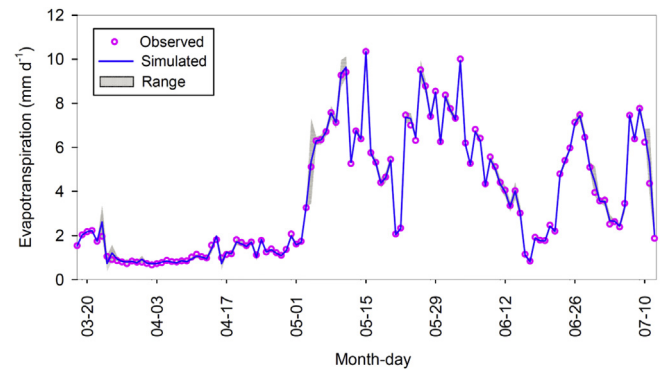

Fig. 5. Simulated versus measured actual evapotranspiration in numerical case. The solid line corresponds to the average simulation of solutions by GPE, while the gray band represents the simulation uncertainty.

Table 6
Goodness-of-fit test indicators of observed and simulated values for numerical case and real experimental case.

Numerical case

	Item	MRE (%)	RMSE	NSE	R^2
	Soil water content (cm^3 cm^{-3})	−0.246	0.006	0.985	0.993
	Salinity concentration (g L^{-1})	−0.210	0.112	0.997	0.999
	ET_a (cm)	−0.300	0.147	0.997	0.997

Experimental case

	Item	MRE (%)	RMSE	NSE	R^2
Calibration (2007)	Soil water content (cm^3 cm^{-3})	−1.200	0.022	0.827	0.842
	Salinity concentration (g L^{-1})	−5.300	1.967	0.292	0.392
	LAI (−)	−3.453	0.429	0.920	0.931
Validation (2008)	Soil water content (cm^3 cm^{-3})	3.373	0.027	0.757	0.809
	Salinity concentration (g L^{-1})	3.199	2.334	0.498	0.569
	LAI (−)	9.060	0.510	0.887	0.903

had only slight effects on model output, especially for the lower two soil layers in this case. The quantitative sensitivity information could be very useful to model calibration.

The parameters to be inversely calibrated were generated from the "very important" and "important" parameters (ranking 1–19 in Table 4). However, the parameters that have little uncertainty or could be known precisely were not necessarily to be calibrated.

Thus, 14 parameters related to soil hydraulic properties, solute transport and salt stress were selected in the following inverse calibration (see Table 5). Five crop growth parameters (T_b, PHU, DLAI, L_{max} and RLAD) were not considered and were set the same values as in Xu et al. (2013), because they were more well-known and had small influences on soil water and solute transport.

3.3. Parameter estimation in case study

3.3.1. Numerical case

Five most probable solutions (i.e. parameter groups) were obtained through inverse simulation in numerical case (Table 5). Figs. 4 and 5 showed the comparison of simulated and observed ET_a, soil moisture and salinity concentration based on inverse modeling. The fitness indicators are given in Table 6. Results showed that the simulated values were almost completely fitted with the observed values (ET_a, RMSE = 0.147 mm, NSE = 0.997; soil moisture, RMSE = 0.006 cm^3 cm^{-3}, NSE = 0.985; soil salinity concentration, RMSE = 0.112 g L^{-1}, NSE = 0.997). Meanwhile, MAE were found to approach zero and R^2 were larger than 0.99 for all output. The values of calibrated parameters are presented in Table 5. The value range almost covered the target (real) values while the average values for most calibrated parameters were approaching to the target values. It was also found that parameters with high sensitivity were much closer to the target values, such as
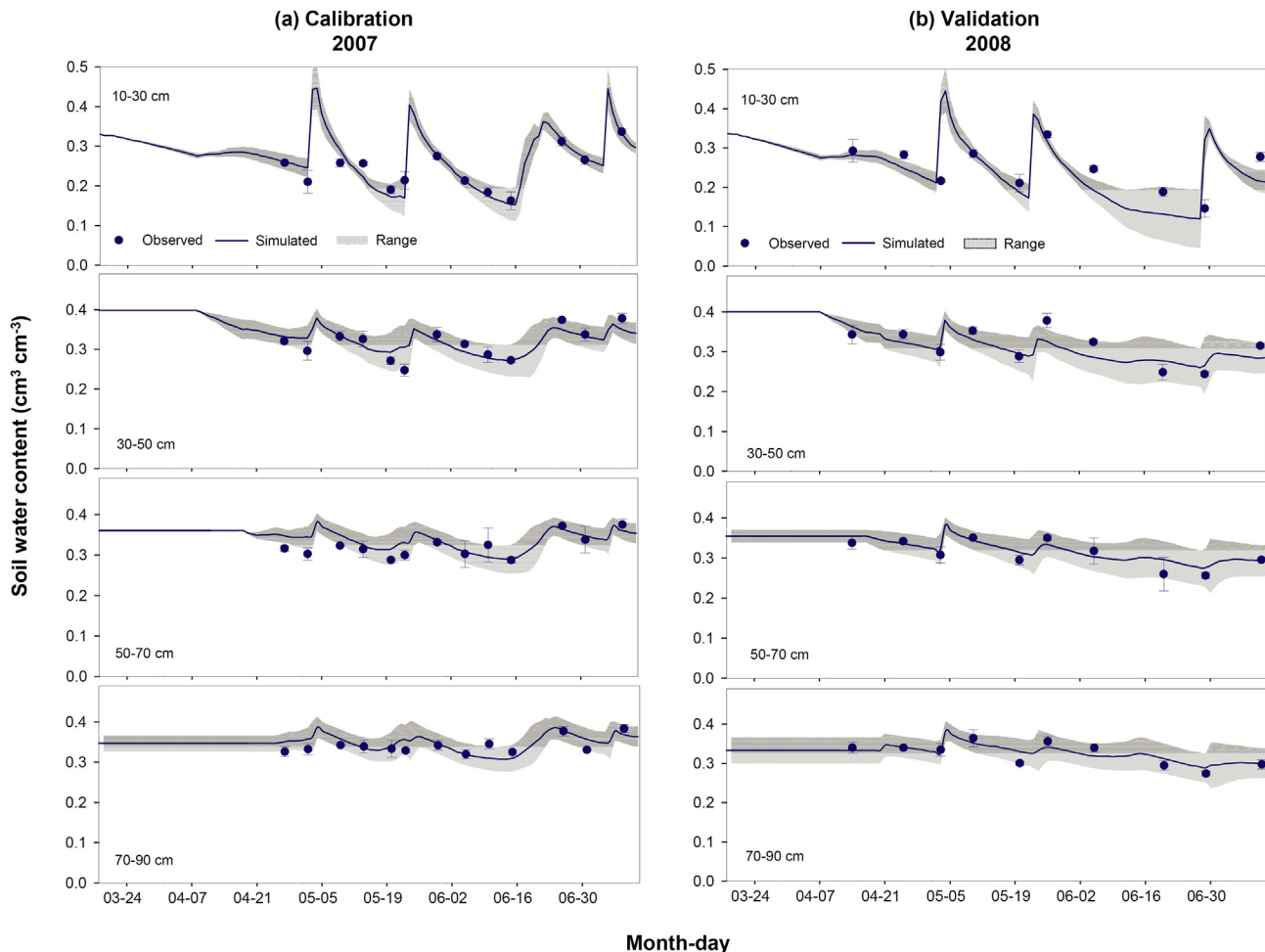

Fig. 6. Simulated versus measured soil water contents in different soil layers during model calibration (a, at left) and validation (b, at right) in the real experimental case. The solid line corresponds to the average simulation of solutions by GPE, while the gray band represents the simulation uncertainty.

α_1, α_2 and L_{dis}. However, the parameter range might also have an impact on the accuracy of inverse estimation. For example, the accuracy of inverse estimation for the most important parameters θ_{s2} was not the highest. Some parameters were more uncertain and difficult to estimate such as K_{s2} that had relatively low sensitivity. The uncertainty bound for simulated ET_a, soil moisture and salinity concentration is presented in Figs. 4 and 5, respectively. There were very small uncertainties for all model output. In summary, the estimated and targeted values for 14 selected parameters were very close with each other, and the simulated data matched very well with observed daily data with some small uncertainties. Thus, the numerical case showed that the GPE module had a potential ability for inverse parameter estimation for agro-hydrological model.

3.3.2. Experimental case

Eight probable solutions were obtained by inverse calibration using 2007 data in field experimental case (Table 5). The simulated soil moisture showed good agreement with the measured values for various soil layers during model calibration in 2007 (Fig. 6a). It produced a RMSE = 0.022 cm^3 cm^{-3}, a NSE = 0.827 and a R^2 = 0.842, which showed a better fitness than that by Xu et al. (2013) with manual try-and-error method. Fig. 7a also shows that the simulated and observed salinity concentration for the same soil layers matched with each other during the calibration period. In addition, Figs. 6a and 7a showed that the predicted uncertainty bounds covered most of the observed values. However, there were

some discrepancies for deeper soil layers (i.e. 50–70 cm and 70–90 cm) that were partly affected by water table fluctuations. This could be related to the low observation frequency of groundwater depths (every 10 days) as well as observation quality (especially for salinity concentration). The LAI values were also simulated in agreement with observations (Fig. 8a), and the fitness results (i.e. RMSE = 0.429, NSE = 0.920 and R^2 = 0.931) were superior to the manual calibration. Note that the simulated soil moisture and LAI were closer to the observed values than soil salinity concentration. This should be the result of the quality of observational data for salinity concentration was worse than the other two. It affected the accuracy of inverse parameter estimation.

The model with calibrated parameters was further tested using the 2008 experimental data. Soil moisture reproduced by the SWAP-EPIC model (Fig. 6b) represented well the observations as shown in the small errors of the estimates (RMSE = 0.027 cm^3 cm^{-3}, NSE = 0.757 and R^2 = 0.809). The simulated salinity concentration was also in agreement with observations (Fig. 7b) (RMSE = 2.334 g L^{-1}, NSC = 0.498 and R^2 = 0.569). In addition, most of the observed data were located in the uncertainty bands for soil moisture and salinity concentration. The performance indicators showed that the accuracy for soil water and salinity was better than that obtained by manual method in Xu et al. (2013). The simulated LAI was also closer to observed values (Table 6). The uncertainty bound was relatively small for LAI and soil salinity concentration. These results indicated an acceptably
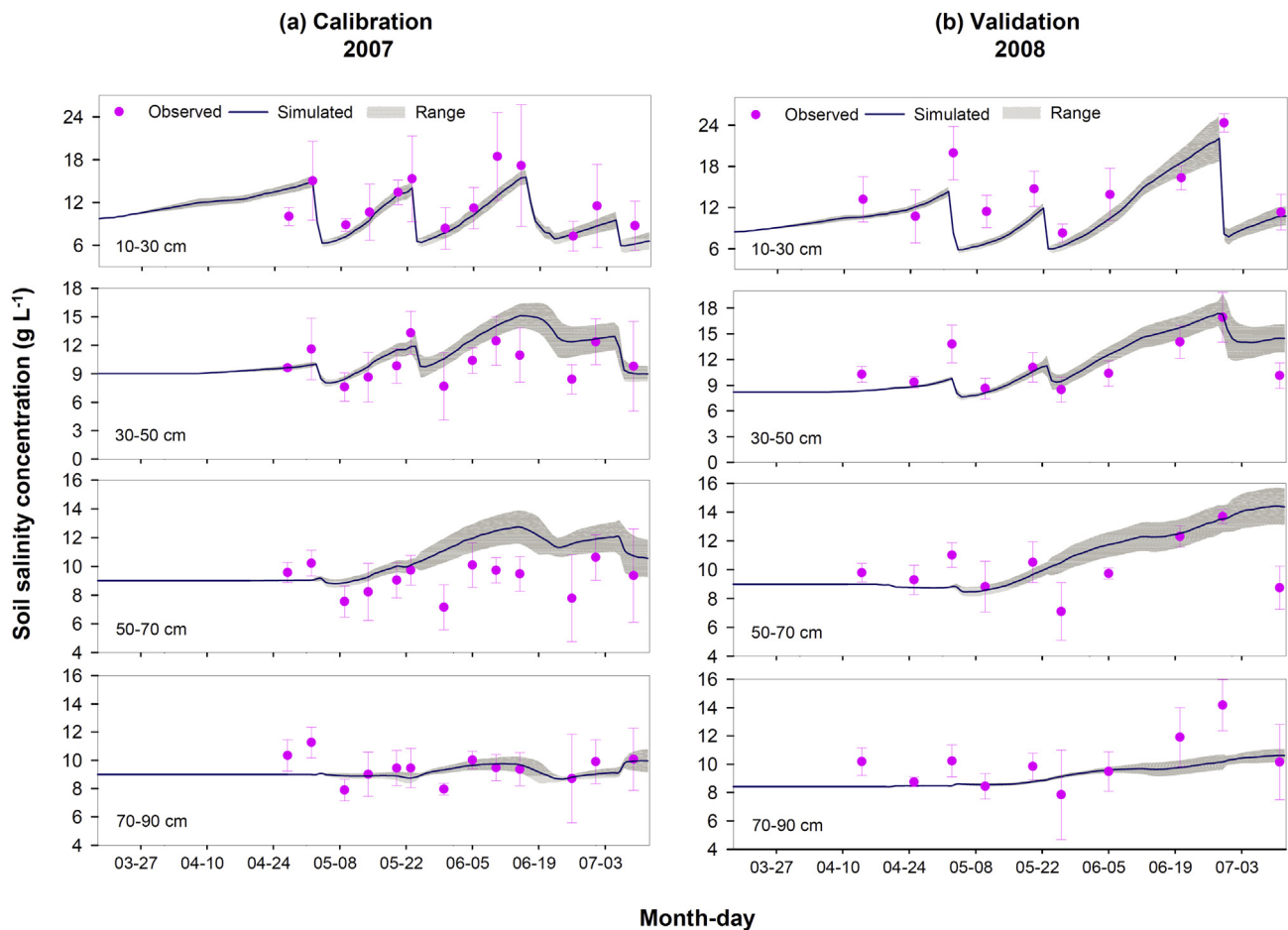

Fig. 7. Simulated versus measured salt content of the soil solution in different soil layers during model calibration (a, left) and validation (b, at right) in the real experimental case. The solid line corresponds to the average simulation of solutions by GPE, while the gray band represents the simulation uncertainty.
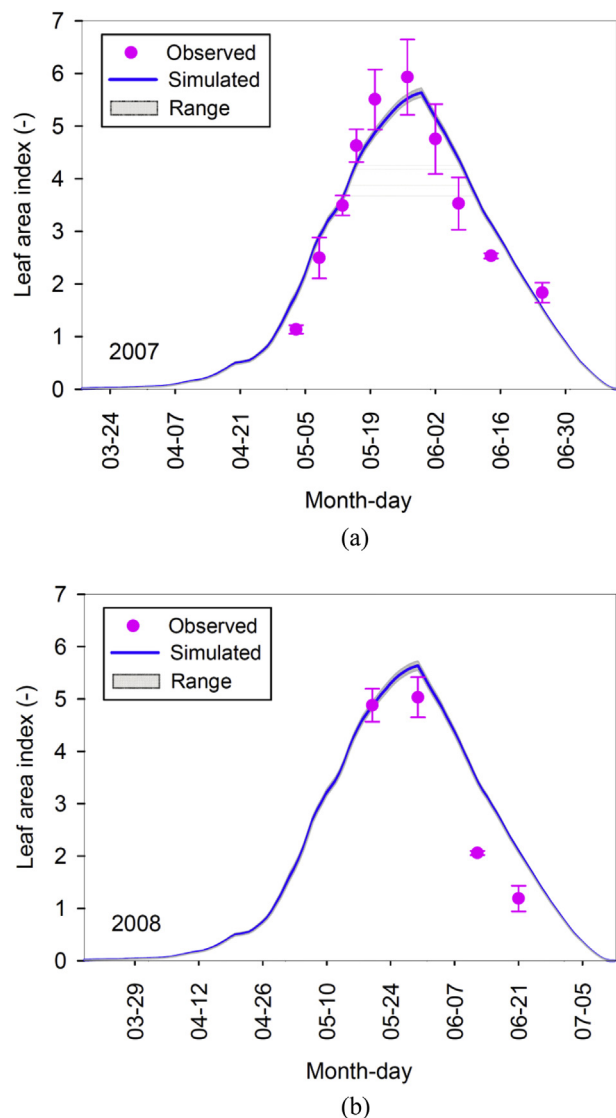
Fig. 8. Simulated versus measured leaf area index during model calibration (a, left) and validation (b, at right) in the real experimental case. The solid line corresponds to the average simulation of solutions by GPE, while the gray band represents the simulation uncertainty.

good simulation of all processes during validation period with the calibrated parameters by the GPE module. The two case studies above showed that the GPE module was useful to inversely calibrate the parameters for an agro-hydrological model. The effects of parameter estimation for numerical case were much better than that for experimental case, due to the good quality of (synthetic) observation. The estimated parameter had larger uncertain range in field experimental case (Table 5). However, the fitness of simulated/observed data was still slightly better than that using the laborious and tedious try-and-error method. In addition, the uncertainties both for parameters and output could be provided when using the GPE module. Thus, this indicated that the GPE method has a good possibility for real field use, but its successful use should be based largely on the quality of the observation data.

In summary, the case studies showed the applicability of the joint use of the GSA and GPE modules. However, some limitations or caveats should also be mentioned, such as: (1) the ranges of

parameters were subjectively defined according to users' experiences, which could influence analysis results for GSA and GPE; (2) the uncertainty for setting the weighting factor ω_k in Eq. (6), which could affect the GPE results for multi-objective problems; (3) the application effects of methods was dependent on the quality of observation data.

4. Conclusion

In this study, the global method of sensitivity analysis and inverse parameter estimation was introduced for a physically-based agro-hydrological model−SWAP-EPIC. The global sensitivity analysis (GSA) module and global parameter estimation (GPE) module were developed based on LH-OAT method and modified-MGA method, respectively. They were well tested and validated with the numerical and field experimental cases, using the experimental data of wheat in an arid irrigation district of Northwest China. This study has well extended the parameter identification to include more processes (i.e. solute transport, root water uptake and crop growth) for the complicated physically-based models. In addition, a new solute transport module was developed for SWAP-EPIC using the fully implicit and Crank-Nicholson finite-difference schemes. It indeed improved the numerical stability of SWAP-EPIC and made it stable enough for GSA and GPE simulation.

The GSA performance showed that only a few parameters were sensitive to the dynamics of agro-hydrological processes in the field case simulation, i.e., only 14 sensitive parameters were found and selected for calibration within 49 parameters. These sensitive parameters were mainly related to the processes of soil water flow, solute transport and salt stress of root water uptake. Results also implied that the sensitivity should be quite close to the specific field conditions. The GPE simulation in the numerical case showed that the searched value range covered the target (real) values and the average values for most calibrated parameters were approaching to their target values. The full consistency between simulated/ observed data further validated the applicability of GPE module. Note that parameters with high sensitivity also have larger probability to reach the real values. Meanwhile, the acceptable agreement of simulated/observed data in the actual experimental case showed the practical applicability in fields. The parameter uncertainty showed that there was relatively larger uncertain range in experimental case than in numerical case. Thus the successful use of GPE module was also affected by the quality of observation data.

In summary, this study presented the potential application of GSA and GPE modules for parameter identification of physically-based agro-hydrological models. While it should pay attention to the effects of parameter ranges, weighting factor of multi-objectives, quality of observation data on the identification results. This will be further studied in our follow-up investigations.

Appendix A. Supplementary data

Supplementary data related to this article can be found at http:// dx.doi.org/10.1016/j.envsoft.2016.05.013.

References

Abbaspour, K.C., Schulin, R., van Genuchten, M.T., 2001. Estimating unsaturated soil hydraulic parameters using ant colony optimization. Adv. Water Resour. 24 (8), 827–841.

Abbaspour, K.C., Johnson, C.A., van Genuchten, M.T., 2004. Estimating uncertain flow and transport parameters using a sequential uncertainty fitting procedure. Vadose Zone J. 3 (4), 1340–1352.

Allen, R.G., Pereira, L.S., Raes, D., Smith, M., 1998. Guidelines for Computing Crop Water Requirements. Crop evapotranspiration, FAO, Rome, Italy. Irrigation and Drainage Paper =56.

Batu, V., 2005. Applied Flow and Solute Transport Modeling in Aquifers: Fundamental Principles and Analytical and Numerical Methods. CRC Press.

Black, T.A., Gardner, W.R., Thurtell, G.W., 1969. The prediction of evaporation, drainage, and soil water storage for a bare soil. Soil Sci. Soc. Am. J. 33 (5), 655–660.

Boesten, J., Stroosnijder, L., 1986. Simple model for daily evaporation from fallow tilled soil under spring conditions in a temperate climate. Neth J. Agric. Sci. 34, 75–90.

Boesten, J.J.T.I., van der Linden, A.M.A., 1991. Modeling the influence of sorption and transformation on pesticide leaching and persistence. J. Environ. Qual. 20 (2), 425–435.

Borg, H., Grimes, D.W., 1986. Depth development of roots with time: an empirical description. Trans. ASAE 29 (1), 194–197.

Campolongo, F., Cariboni, J., Saltelli, A., 2007. An effective screening design for sensitivity analysis of large models. Environ. Modell. Softw. 22 (10), 1509–1518.

Cariboni, J., Gatelli, D., Liska, R., Saltelli, A., 2007. The role of sensitivity analysis in ecological modeling. Ecol. Modell. 203 (1–2), 167–182.

Carroll, D.L., 1998. GA Fortran Driver Version 1.7 [EB/OL]. http://www.cuaerospace.com/carroll/ga.html.

DeJonge, K.C., Ascough II, J.C., Ahmadi, M., Andales, A.A., Arabi, M., 2012. Global sensitivity and uncertainty analysis of a dynamic agroecosystem model under different irrigation treatments. Ecol. Modell. 231, 113–125.

Della Peruta, R., Keller, A., Schulin, R., 2014. Sensitivity analysis, calibration and validation of EPIC for modelling soil phosphorus dynamics in Swiss agro-ecosystems. Environ. Modell. Softw. 62, 97–111.

Dirksen, C., Augustijn, D.C., 1988. Root Water Uptake Function for Nonuniform Pressure and Osmotic Potentials. ASA, Madison, WI, 185. Agronomy Abstract.

Duan, Q., Sorooshian, S., Gupta, V.K., 1994. Optimal use of the SCE-UA global optimization method for calibrating watershed models. J. Hydrol. 158 (3–4), 265–284.

Easterling, W.E., Rosenberg, N.J., McKenney, M.S., Jones, C.A., Dyke, P.T., Williams, J.R., 1992. Preparing the erosion productivity impact calculator (EPIC) model to simulate crop response to climate change and the direct effects of CO_2. Agric. Meteorol. 59 (1–2), 17–34.

Evensen, G., 2003. The Ensemble Kalman filter: theoretical formulation and practical implementation. Ocean. Dyn. 53 (4), 343–367.

Goldberg, D.E., 1989. Genetic Algorithms in Search, Optimization and Machine Learning. Addison-Wesley, Reading, Mass.

Goldberg, D.E., 2002. The Design of Innovation: Lessons from and for Competent Genetic Algorithms. Springer Science & Business Media.

Hamby, D.M., 1994. A review of techniques for parameter sensitivity analysis of environmental models. Environ. Monit. Assess. 32 (2), 135–154.

Holland, J.H., 1975. Adaptation in Natural and Artificial Systems, Edited. University of Michigan Press, Ann Arbor.

Hu, Y., Garcia-Cabrejo, O., Cai, X., Valocchi, A.J., DuPont, B., 2015. Global sensitivity analysis for large-scale socio-hydrological models using Hadoop. Environ. Modell. Softw. 73, 231–243.

Hupet, F., Lambot, S., Feddes, R.A., van Dam, J.C., Vanclooster, M., 2003. Estimation of root water uptake parameters by inverse modeling with soil water content data. Water Resour. Res. 39 (11), 1312.

Ines, A.V., Mohanty, B.P., 2008. Near-surface soil moisture assimilation for quantifying effective soil hydraulic properties using genetic algorithm: 1. Conceptual modeling. Water Resour. Res. 44, W06422. http://dx.doi.org/10.1029/2007WR005990.

Ines, A.V.M., Droogers, P., 2002. Inverse modelling in estimating soil hydraulic functions: a Genetic Algorithm approach. Hydrol. Earth Syst. Sci. 6 (1), 49–66.

Jacques, D., Šimůnek, J., Timmerman, A., Feyen, J., 2002. Calibration of Richards' and convection–dispersion equations to field-scale water flow and solute transport under rainfall conditions. J. Hydrol. 259 (1–4), 15–31.

Jiang, Y., Xu, X., Huang, Q., Huo, Z., Huang, G., 2015. Assessment of irrigation performance and water productivity in irrigated areas of the middle Heihe River basin using a distributed agro-hydrological model. Agric. Water Manage 147, 67–81.

Jones, C.A., 1985. C4 Grasses and Cereals. John Wiley and Sons, Inc., New York, p. 412.

Kool, J.B., Parker, J.C., van Genuchten, M.T., 1987. Parameter estimation for unsaturated flow and transport models—A review. J. Hydrol. 91 (3–4), 255–293.

Kroes, J.G., van Dam, J.C., 2003. Reference Manual SWAP Version 3.0.3. Alterra, Green World Research, Wageningen, p. 211. Alterra-report 773.

Lindstrom, F.T., Haque, R., Freed, V.H., Boersma, L., 1967. The movement of some herbicides in soils. Linear diffusion and convection of chemicals in soils. Environ. Sci. Technol. 1 (7), 561–565.

Malone, R.W., Jaynes, D.B., Ma, L., Nolan, B.T., Meek, D.W., Karlen, D.L., 2010. Soil-test N recommendations augmented with PEST-optimized RZWQM simulations. J. Environ. Qual. 39 (5), 1711–1723.

Monsi, M., Saeki, T., 1953. Uber den Lictfaktor in den Pflanzengesellschaften und sein Bedeutung fur die Stoffproduktion. Jpn. J. Bot. 14, 22–52.

Monteith, J.L., 1965. Evaporation and the environment. In: The State and Movement of Water in Living Organisims. Cambridge University Press, Swansea, pp. 205–234.

Monteith, J.L., Moss, C.J., 1977. Climate and the efficiency of crop production in britain [and discussion]. Philosophical transactions of the royal society of London. B, Biol. Sci. 281 (980), 277–294.

Moriasi, D.N., Arnold, J.G., Van Liew, M.W., Bingner, R.L., Harmel, R.D., Veith, T.L., 2007. Model evaluation guidelines for systematic quantification of accuracy in watershed simulations. Trans. ASABE 50 (3), 885–900.

Mualem, Y., 1976. A new model for predicting the hydraulic conductivity of unsaturated porous media. Water Resour. Res. 12 (3), 513–522.

Neelam, M., Mohanty, B.P., 2015. Global sensitivity analysis of the radiative transfer model. Water Resour. Res. 51 (4), 2428–2443.

Nossent, J., Elsen, P., Bauwens, W., 2011. Sobol' sensitivity analysis of a complex environmental model. Environ. Modell. Softw. 26 (12), 1515–1525.

Paredes, P., Rodrigues, G.C., Alves, I., Pereira, L.S., 2014. Partitioning evapotranspiration, yield prediction and economic returns of maize under various irrigation management strategies. Agric. Water Manage 135, 27–39.

Pianosi, F., Sarrazin, F., Wagener, T.A., 2015. Matlab toolbox for global sensitivity analysis. Environ. Modell. Softw. 70, 80–85.

Ranatunga, K., Nation, E.R., Barratt, D.G., 2008. Review of soil water models and their applications in Australia. Environ. Modell. Softw. 23 (9), 1182–1206.

Saltelli, A., Tarantola, S., Chan, K., 1999. A quantitative model-independent method for global sensitivity analysis of model output. Technometrics 41 (1), 39–56.

Saltelli, A., Annoni, P., 2010. How to avoid a perfunctory sensitivity analysis. Environ. Modell. Softw. 25 (12), 1508–1517.

Sarrazin, F., Pianosi, F., Wagener, T., 2016. Global sensitivity analysis of environmental models: convergence and validation. Environ. Modell. Softw. 79, 135–152.

Shafiei, M., Ghahraman, B., Saghafian, B., Davary, K., Pande, S., Vazifedoust, M., 2014. Uncertainty assessment of the agro-hydrological SWAP model application at field scale: a case study in a dry region. Agric. Water Manage 135, 324–334.

Shin, Y., Mohanty, B.P., Ines, A.V.M., 2012. Soil hydraulic properties in one-dimensional layered soil profile using layer-specific soil moisture assimilation scheme. Water Resour. Res. 48, W06529. http://dx.doi.org/10.1029/2010WR009581.

Šimůnek, J., van Genuchten, M.T., 1996. Estimating unsaturated soil hydraulic properties from tension disc infiltrometer data by numerical inversion. Water Resour. Res. 32 (9), 2683–2696.

Šimůnek, J., Huang, K., van Genuchten, M.T., 1997. The HYDRUS-et software package for simulating the one-dimensional movement of water, heat and multiple solutes in variably-saturated media. In: Bratislava: Inst. Hydrology, Slovak Acad. Sci, p. 184. Version 1.1.

Stockle, C.O., Williams, J.R., Rosenberg, N.J., Jones, C.A., 1992. A method for estimating the direct and climatic effects of rising atmospheric carbon dioxide on growth and yield of crops: Part I—Modification of the EPIC model for climate change analysis. Agric. Syst. 38 (3), 225–238.

van Dam, J.C., Huygen, J., Wesseling, J.G., Feddes, R.A., Kabat, P., van Walsum, P.E.V., Groenendijk, P., van Diepen, C.A., 1997. Theory of SWAP Version 2.0. Simulation of Water Flow, Solute Transport and Plant Growth in the Soil–water–atmosphere–plant Environment. DLO Winand Staring Centre-DLO, p. 167. Department of water resources, WAU, Report 71, technical Document 45.

van Dam, J.C., Groenendijk, P., Hendriks, R.F.A., Kroes, J.G., 2008. Advances of modeling water flow in variably saturated soils with SWAP. Vadose Zone J. 7 (2), 640–653.

van Genuchten, M.T., Wierenga, P.J., 1974. Simulation of One-dimensional Solute Transfer in Porous Media. New Mexico Agricultural Experiment Station Bulletin 628, Las Cruces, N.M.

van Genuchten, M.T., 1980. A closed-form equation for predicting the hydraulic conductivity of unsaturated soils. Soil Sci. Soc. Am. J. 44 (5), 892–898.

van Griensven, A., Meixner, T., Grunwald, S., Bishop, T., Diluzio, M., Srinivasan, R., 2006. A global sensitivity analysis tool for the parameters of multi-variable catchment models. J. Hydrol. 324 (1–4), 10–23.

Varella, H., Guérif, M., Buis, S., 2010. Global sensitivity analysis measures the quality of parameter estimation: the case of soil parameters and a crop model. Environ. Modell. Softw. 25 (3), 310–319.

Wesseling, J.G., Kroes, J.G., Metselaar, K., 1998. Global Sensitivity Analysis of the Soil-water-atmosphere-plant (SWAP) Model. DLO-Staring Centre, p. 70. Report 160.

Williams, J.R., Jones, C.A., Kiniry, J.R., Spanel, D.A., 1989. The EPIC crop growth model. Trans. ASAE 32 (2), 497–511.

Wöhling, T., Vrugt, J.A., Barkle, G.F., 2008. Comparison of three multiobjective optimization algorithms for inverse modeling of vadose zone hydraulic properties. Soil Sci. Soc. Am. J. 72 (2), 305–319.

Xu, X., Qu, Z., Huang, G., 2012. Optimization of soil hydraulic and solute transport parameters using genetic algorithms at field scale. Shuili Xuebao J. Hydraul. Eng. 43 (7), 808–815.

Xu, X., Huang, G., Sun, C., Pereira, L.S., Ramos, T.B., Huang, Q., Hao, Y., 2013. Assessing the effects of water table depth on water use, soil salinity and wheat yield: searching for a target depth for irrigated areas in the upper Yellow River basin. Agric. Water Manage 125, 46–60.

Xu, X., Sun, C., Qu, Z., Huang, Q., Ramos, T.B., Huang, G., 2015. Groundwater recharge and capillary rise in irrigated areas of the upper Yellow River basin assessed by an agro-Hydrological model. Irrig. Drain. http://dx.doi.org/10.1002/ird.1928.

Yang, J., 2011. Convergence and uncertainty analyses in Monte-Carlo based sensitivity analysis. Environ. Modell. Softw. 26 (4), 444–457.

Yang, J., Reichert, P., Abbaspour, K.C., Xia, J., Yang, H., 2008. Comparing uncertainty analysis techniques for a SWAT application to the Chaohe Basin in China. J. Hydrol. 358 (1), 1–23.

Zhao, G., Bryan, B.A., Song, X., 2014. Sensitivity and uncertainty analysis of the APSIM-wheat model: interactions between cultivar, environmental, and management parameters. Ecol. Modell. 279, 1–11.

Zheng, C., Bennett, G.D., 2002. Applied Contaminant Transport Modeling. Wiley-Interscience, New York.